



## King's Research Portal

DOI:

[10.2967/jnumed.116.177741](https://doi.org/10.2967/jnumed.116.177741)

*Document Version*

Peer reviewed version

[Link to publication record in King's Research Portal](#)

*Citation for published version (APA):*

van der Meer, L., Terry, S. Y. A., van Ingen Schenau, D., Andree, K., Franssen, G., Roeleveld, D., Metselaar, J., Reinheckel, T., Hoogerbrugge, P., Boerman, O., & van Leeuwen, F. (2016). In vivo imaging of antileukemic drug asparaginase reveals a rapid macrophage mediated clearance from the bone marrow. *Journal of Nuclear Medicine*. Advance online publication. <https://doi.org/10.2967/jnumed.116.177741>

### **Citing this paper**

Please note that where the full-text provided on King's Research Portal is the Author Accepted Manuscript or Post-Print version this may differ from the final Published version. If citing, it is advised that you check and use the publisher's definitive version for pagination, volume/issue, and date of publication details. And where the final published version is provided on the Research Portal, if citing you are again advised to check the publisher's website for any subsequent corrections.

### **General rights**

Copyright and moral rights for the publications made accessible in the Research Portal are retained by the authors and/or other copyright owners and it is a condition of accessing publications that users recognize and abide by the legal requirements associated with these rights.

- Users may download and print one copy of any publication from the Research Portal for the purpose of private study or research.
- You may not further distribute the material or use it for any profit-making activity or commercial gain
- You may freely distribute the URL identifying the publication in the Research Portal

### **Take down policy**

If you believe that this document breaches copyright please contact [librarypure@kcl.ac.uk](mailto:librarypure@kcl.ac.uk) providing details, and we will remove access to the work immediately and investigate your claim.

# **In vivo imaging of antileukemic drug asparaginase reveals a rapid macrophage mediated clearance from the bone marrow**

Laurens T van der Meer<sup>1\*</sup>, Samantha YA Terry<sup>2,3\*</sup>, Dorette S van Ingen Schenau<sup>1</sup>, Kiki C Andree<sup>1</sup>, Gerben M Franssen<sup>2</sup>, Debbie M Roeleveld<sup>1,4</sup>, Josbert M Metselaar<sup>5</sup>, Thomas Reinheckel<sup>6,7,8</sup>, Peter M Hoogerbrugge<sup>9</sup>, Otto C Boerman<sup>2</sup>, Frank N van Leeuwen<sup>1</sup>

<sup>1</sup>Laboratory of Pediatric Oncology, Radboud Institute for Molecular Life Sciences, Radboud university medical center, Nijmegen, the Netherlands <sup>2</sup> Department of Radiology and Nuclear Medicine, Radboud university medical center, Nijmegen, the Netherlands <sup>3</sup>Department of Imaging Chemistry and Biology, Division of Imaging Sciences and Biomedical Engineering, King's College London, London, United Kingdom <sup>4</sup>Experimental Rheumatology, Radboud Institute for Molecular Life Sciences, Radboud university medical center, Nijmegen, the Netherlands <sup>5</sup>Department of Experimental Molecular Imaging, University Clinic and Helmholtz Institute for Biomedical Engineering, RWTH-Aachen University, Aachen, Germany <sup>6</sup>Institute of Molecular Medicine and Cell Research, Albert-Ludwigs-University, Freiburg, Germany <sup>7</sup>German Cancer Consortium (DKTK), Freiburg, Germany <sup>8</sup>BIOSS Centre for Biological Signalling Studies, Albert-Ludwigs-University, Freiburg, Germany <sup>9</sup>Princess Maxima Center for Pediatric Oncology, Utrecht, the Netherlands

\* L.T.v.d.M. and S.Y.A.T. contributed equally to this study

## **Running title**

Imaging of asparaginase biodistribution and clearance

## **Keywords**

Leukemia, asparaginase, imaging, macrophages, cathepsin B

## **Financial Support**

This work was supported in part by research funding from KiKa (grant #134) (L.T.v.d.M.)

## **Corresponding Author**

Frank N. van Leeuwen

412 Laboratory of Pediatric Oncology,

Radboud university medical center, PO Box 9101,

6500 HB Nijmegen, The Netherlands

+31 (0) 243666203

FrankN.vanleeuwen@radboudumc.nl

## **Conflict of interest disclosure**

The authors have no relevant conflict of interest to declare.

**Word count:** 4859

**Figure count:** 4 figures, 5 supplemental figures

## **Abstract**

The antileukemic drug asparaginase, a key component in the treatment of acute lymphoblastic leukemia, acts by depleting asparagine from the blood. However, little is known about its pharmacokinetics and mechanisms of therapy resistance are poorly understood. Here, we explored the in vivo biodistribution of radiolabeled asparaginase, using a combination of imaging and biochemical techniques, and provide evidence for tissue specific clearance mechanisms, which could reduce effectiveness of the drug at these specific sites.

**Methods.** In vivo localization of Indium-111-labeled *E.coli* asparaginase was carried out in C57Bl/6 mice by both microSPECT/CT and by ex vivo biodistribution studies. Mice were treated with liposomal clodronate to investigate the effect of macrophage depletion on tracer localization and drug clearance in vivo. Moreover, macrophage cell line models RAW264.7 and THP-1, as well as knockout mice, were used to identify the cellular and molecular components controlling asparaginase pharmacokinetics.

**Results.** In vivo imaging and biodistribution studies showed a rapid accumulation of asparaginase in macrophage-rich tissues such as liver, spleen and in particular bone marrow. Clodronate-mediated depletion of phagocytic cells markedly prolonged the serum half-life of asparaginase in vivo and decreased drug uptake in these macrophage rich organs. Immunohistochemistry and in vitro binding assays confirmed the involvement of macrophage-like cells in the uptake of asparaginase. We identified the activity of the lysosomal protease cathepsin B in macrophages as a rate-limiting factor in degrading asparaginase both in vitro and in vivo.

**Conclusion.** We show that asparaginase is rapidly cleared from the serum by liver, spleen and bone marrow-resident phagocytic cells. As a consequence of this efficient uptake and protease mediated degradation, particularly bone marrow resident macrophages may provide a protective niche to leukemic cells.

## Introduction

The therapeutic enzyme asparaginase is an essential component of the multi-drug regimen used in the treatment of children and adults with acute lymphoblastic leukemia (ALL). Upon administration, this drug converts serum asparagine into aspartate, thereby effectively depleting the blood from this amino acid. Unlike most other cells in the body, lymphocytes, including leukemic blasts, are fully dependent on uptake of asparagine from the blood and die as a result of nutrient stress <sup>1</sup>.

The effectiveness of asparaginase treatment relies on the complete depletion of asparagine from the leukemic cell niche. It has been suggested that during asparaginase treatment, leukemic cell survival is supported by asparagine released by surrounding mesenchymal cells <sup>2,3</sup>. Although asparagine levels are significantly higher in bone marrow aspirates when compared to matched blood samples, these levels drop upon treatment with asparaginase <sup>4,5</sup>. However, analyses of aspirates may not accurately reflect asparagine concentrations in situ.

Despite the fact that asparaginase has been a cornerstone of ALL treatment protocols since its introduction in the 1970s, little is known about the fate of the infused asparaginase and the mechanisms that determine the pharmacodynamics of this drug. With a molecular weight of 170 kDa that greatly exceeds the limits for renal filtration (~60 kDa), mononuclear phagocyte system (MPS) based (or reticulo-endothelial) clearance is the suggested mode of degradation <sup>6</sup>.

Furthermore, the intracellular/molecular mechanisms that influence asparaginase pharmacokinetics remain poorly understood. One study showed that the lysosomal cysteine proteases legumain (or Asparagine Endopeptidase (AEP)) and cathepsin B efficiently degrade asparaginase in vitro <sup>7</sup>.

Consistent with these observations, we recently identified a patient carrying a germline mutation in cathepsin B who showed strongly delayed asparaginase degradation <sup>8</sup>. However, further validation of these findings and their clinical implications is needed.

In the present study we used microSPECT/CT imaging to visualize the in vivo distribution of <sup>111</sup>Indium-labeled asparaginase in a mouse model and identified both cellular and molecular components that determine asparaginase pharmacokinetics.

## **Materials and Methods**

### **Mouse models**

All animal experiments were approved by the Animal Experimental Committee of the Radboud university medical center and performed in accordance with institutional and national guidelines. Wildtype C57Bl/6J mice were obtained from Charles River (Leiden, the Netherlands). Cathepsin B knockout mice were described previously<sup>9</sup> and have been backcrossed to C57Bl/6J for 10 generations. All mice were housed in individually ventilated filter-top cages, and a standard diet and water were provided ad libitum. The mice were used between ages 8 and 10 weeks.

### **Micro-SPECT/CT imaging**

Mice were injected intravenously with 3 I.U. / gram of bodyweight of <sup>111</sup>In-DTPA-asparaginase (21-24 MBq/mouse in 200  $\mu$ L, see supplemental methods for labeling procedure) and scanned under anesthesia (isoflurane/O<sub>2</sub>) at indicated time points after injection using the U-SPECT-II/CT ((MILabs, Utrecht, the Netherlands<sup>10</sup>). CT scans (spatial resolution 160  $\mu$ m, 65 kV, 615  $\mu$ A) were acquired for anatomical reference. SPECT scans, (3 frames of 17 min), were reconstructed using an ordered-subset expectation maximization algorithm, with a voxel size of 0.4 mm. SPECT images were analyzed quantitatively as described previously<sup>11</sup>.

### **Biodistribution experiments**

Mice were injected intravenously with 3 I.U. <sup>111</sup>In-DTPA-asparaginase / gram of bodyweight. Mice were euthanized by CO<sub>2</sub>/O<sub>2</sub> asphyxiation at the indicated times after injection. Blood and major organs and tissues were dissected, weighed, and counted in a gamma counter. In addition, organs were used for autoradiography and immunohistochemical analysis (see supplemental methods for procedures).

### **Pharmacokinetics experiments**

Mice were injected intravenously with 3 I.U. Asparaginase/gram of bodyweight (Takeda, Hoofddorp, the Netherlands). At the indicated times after injection, mice were euthanized by CO<sub>2</sub>/O<sub>2</sub> asphyxiation, a blood sample was drawn and tissues of interest were dissected. When indicated, mice were pretreated with 150 µl (1 mg/ml clodronate) liposomes or control liposomes<sup>12</sup> via tail vein injection 24 hours before administration of <sup>111</sup>In-labeled asparaginase. Residual asparaginase activity in serum was determined by photometric detection of the ammonia release after reaction with Nessler's reagent (Sigma-Aldrich, Gorinchem, the Netherlands). In brief, 15 µl serum was diluted with 60 µl 44 mM L-asparagine (Sigma-Aldrich) dissolved in 15 mM Tris-HCl buffer, pH 7.3, supplemented with 0.015% (w/v) BSA and incubated at 37 °C for 30-45 min. The reaction was stopped by the addition of 50 µl trichloroacetic acid (24.5% (w/v), Sigma-Aldrich). After centrifugation 15 µl of the supernatant was added to 120 µl Nessler's solution diluted with deionized water (1:8). The optical density of the solution was measured at 450 nm using the Multiskan Ascent plate reader (MTX Lab systems, Vienna, VA).

### **Cathepsin B activity assay**

Cathepsin B activity was measured using the fluorescent substrate Ac-RR-AFC according to manufacturer's instructions (BioVision, San Francisco, CA). Prism software was used to plot the data and for statistical analysis.  $p < 0.05$  was considered a significant difference.

### **Asparaginase degradation assay**

THP-1 and RAW264.7 cells (see supplemental methods for culture conditions) were lysed by freeze-thawing in degradation buffer (50 mM trisodium citrate buffer, pH 4.5, 5 mM DTT), cleared by centrifugation. For each timepoint, 5 I.U./ml asparaginase was incubated in lysate containing 20 µg of protein. Where indicated, 1 µM Ca-074 (Sigma-Aldrich) was added to inhibit cathepsin B activity. After incubation, asparaginase activity was determined by photometric detection of the ammonia release after reaction with Nessler's reagent using the Multiskan Ascent plate reader as described



above. Prism software was used to plot the data and for statistical analysis. ANOVA was used to test for significance;  $p < 0.05$  was considered a significant difference.

#### **shRNA mediated knockdown**

For lentiviral transduction, HEK293FT cells were transfected with one lentiviral pLKO.1-puro vector (Dharmacon / GE Healthcare), see Supplemental Table 1 for shRNA sequences) together with pVSV-G and psPAX2 using Lipofectamine 2000 (Invitrogen). THP-1 cells were transduced in the presence of  $8\mu\text{g/mL}$  polybrene and 24 hours after transduction selected with  $1\mu\text{g/mL}$  puromycin (Sigma-Aldrich).

**See supplemental method section for details on the asparaginase binding assay, immunoblotting and RT-qPCR.**

## Results

### *MicroSPECT/CT and biodistribution of Asparaginase*

To gain more insight into the in vivo distribution of asparaginase and its degradation, we injected mice with  $^{111}\text{In}$ -labeled asparaginase and monitored its biodistribution (Figure 1, Supplemental Movie 1). Imaging (Figure 1A) and ex vivo biodistribution (Figure 1B) data showed similar trends. Two hours after injection, asparaginase was mainly present in the circulation ( $15.8 \pm 1.4$  %ID/g). However, already at this time point we observed accumulation in the liver ( $8.5 \pm 0.4$  %ID/g) and spleen ( $21.1 \pm 3.6$  %ID/g), the organs in which a large part of the phagocytic cells reside that make up the MPS (Figure 1B). Additionally, we observed that a significant part of radiolabeled asparaginase label rapidly localized to the skeleton (femur at 2 hours post injection:  $13.0 \pm 4.0$  %ID/g), suggesting active uptake by bone marrow resident cells. Over time, the radiolabeled drug levels decreased in the blood pool, but drug uptake in the femur remained stable (at 19 hours post injection:  $14.6 \pm 1.7$  %ID/g) and increased in the spleen ( $42.1 \pm 15.9$  %ID/g) and liver ( $10.5 \pm 1.5$  %ID/g). (Figure 1B).

Quantitative SPECT analysis revealed an almost identical in vivo distribution as determined by ex vivo biodistribution (Figure 1C, Supplemental Figure 1). For instance, radiolabeled asparaginase cleared rapidly from the blood and increased in the spleen over time ( $7.9 \pm 1.9$  %ID/g and  $13.8 \pm 3.8$  %ID/g at 2 and 19h post injection, respectively). Uptake of  $^{111}\text{In}$ -asparaginase in the femur and sternum remained unaltered at 2 ( $10.1 \pm 2.4$  %ID/g) and 19h ( $11.5 \pm 2.0$  %ID/g) post injection. Quantitative SPECT data and biodistribution data correlated well as shown in Figure 1D (Spearman  $r$  at 0.7996). Autoradiography (Supplemental Figure 2A) and immunohistochemical analysis using anti-asparaginase antibodies (Supplemental Figure 2B) were used to study asparaginase localization in more detail. This revealed accumulation of asparaginase in the bone marrow in spinal cord and hind legs. Uptake in the spleen was restricted to the macrophage-rich structure known as red pulp. The accumulation of asparaginase in the kidney was limited to the cortex of this organ, consistent with glomerular entrapment. The asparaginase immune stainings showed a similar pattern to that of the

macrophage marker F4/80 , suggesting that macrophage-like cells are responsible for the uptake. Together these results point towards a crucial role for phagocytic cells in liver, spleen and bone marrow in the clearance of asparaginase.

#### *Macrophage depletion by clodronate liposomes disrupts asparaginase biodistribution*

To further study the role of phagocytic cells for asparaginase biodistribution and turnover, we used clodronate liposomes to deplete phagocytic cells from the organs of interest. We observed an almost complete depletion of F4/80 positive macrophages in liver and spleen and a marked decrease of the numbers of macrophages in bone marrow (Supplemental Figure 3) 24 hours after injection of clodronate liposomes. Clodronate pretreatment significantly prolonged the serum half-life of asparaginase (Figure 2A). MicroSPECT/CT (Figure 2B and Supplemental Movie 2) and ex vivo biodistribution assays (Figure 2C) confirmed that clodronate pre-treatment markedly affected the in vivo distribution of asparaginase. SPECT scans of control mice were similar to those obtained in previous experiments (data not shown). In contrast, in clodronate-treated mice, asparaginase was still detectable in the circulation, while little activity was observed in liver ( $2.5 \pm 0.4$  %ID/g) and spleen ( $3.2 \pm 0.5$  %ID/g), indicating a near complete block in asparaginase uptake by these organs. Furthermore, accumulation in the bone marrow was significantly diminished (femur:  $7.2 \pm 4.5$  %ID/g; spine:  $2.2 \pm 0.5$  %ID/g; sternum:  $2.8 \pm 0.9$  %ID/g), which is consistent with the partial depletion of macrophages in this tissue (Supplemental Figure 3e,f). Together our results establish a central role for phagocytic cells in the regulation of asparaginase pharmacokinetics.

#### *Assessment of the biological clearance mechanism*

Our data indicate highly efficient uptake of asparaginase by murine phagocytic cells. To determine whether these findings could be replicated with human cells, we incubated freshly isolated PBMCs from healthy volunteers with FITC-labeled asparaginase and used flow cytometry to assess which cells bind/internalize asparaginase. Consistent with our observations in mice, predominantly cells

expressing the monocyte/macrophage marker CD14 ( $76.4 \pm 14.8 \%$ ) were found to bind asparaginase (Figure 3B).

In an earlier study, we identified lysosomal protease cathepsin B as a critical determinant of asparaginase half-life<sup>8</sup>. In order to link this observation to the potential role for phagocytic cells identified here, we studied the role of cathepsin B in macrophage-mediated degradation of asparaginase. To this end, we used THP-1 cells, a human monocytic cell line that can be forced into differentiation towards a macrophage like phenotype using phorbol-12-myristate-13-acetate (PMA). Similar to freshly isolated CD14+ cells, THP-1 cells efficiently bound asparaginase (Supplemental Figure 4). We used a previously described in vitro degradation assay<sup>8</sup> to show that asparaginase activity remained unaffected in the monocyte lysate, while the protein was rapidly degraded in lysates from differentiated cells. We observed a similar, but even more efficient degradation in lysates of the murine macrophage cell line RAW264.7. Importantly, degradation in both macrophage lysates was completely inhibited by the addition of the cathepsin B inhibitor CA-074 (Figure 3C, red marked values).

To investigate the correlation between cathepsin B expression and asparaginase degradation, we compared cathepsin B mRNA expression levels in undifferentiated versus differentiated THP-1 cells, (Figure 4A) and found that cathepsin B mRNA expression is strongly induced upon differentiation. RNAi mediated suppression of cathepsin B activity (Figure 4B and Supplemental Figure 5A and B) resulted in a complete or partial block of asparaginase degradation, depending on knockdown efficiency (Figure 4C). Furthermore, we observed that the serum half-life of asparaginase was strongly prolonged in cathepsin B knockout mice compared (Figure 4D). Together, these data firmly establish that cathepsin B activity is an essential and a rate-limiting enzyme for asparaginase degradation by macrophages.

## Discussion

Although asparaginase has been used for decades in the treatment of patients with ALL, little is known about its metabolic fate in patients. Although depletion of asparagine in serum and bone marrow aspirates can be monitored and shows complete depletion when asparaginase concentrations reach threshold levels, concentrations in situ and the supportive role of the microenvironment are subject of debate<sup>2, 3, 5, 13-16</sup>. The question remains whether asparaginase is sufficiently active at this particular niche where the leukemia originates and where leukemia-initiating cells reside.

We applied in vivo imaging of radiolabeled asparaginase with microSPECT/CT to visualize asparaginase biodistribution. In addition to spleen and liver, both organs most frequently involved in uptake of foreign (macro)molecules and particles, we found a remarkably rapid and strong accumulation of asparaginase in the bone marrow. Although bone marrow resident macrophages are part of the MPS, the role of these cells in clearing the blood from macromolecules is often secondary to spleen and liver resident cells and is directed by the size of the molecule<sup>17, 18</sup>. Because for its therapeutic action, asparaginase needs to be present in the serum, this raises the question whether rapid clearance of the drug by bone marrow resident macrophages will negatively affect the depletion of asparagine in the bone marrow niche. Hence, our imaging approach may reflect a rapid local elimination of the drug that could provide a mechanism by which leukemic cells can escape from apoptosis as a result of the asparaginase induced nutrient limitation.

Only a few studies have addressed the potential molecular mechanisms involved in the regulation of asparaginase kinetics. We show a highly efficient uptake of asparaginase by phagocytic cells, predominantly macrophages. These cells express a large variety of antigen uptake receptors that recognize macromolecules based on charge, peptide structure or modification, which are subsequently internalized and degraded in the endosomal compartment<sup>19</sup>. Previous reports discuss

the role of lysosomal proteases in controlling asparaginase degradation in vitro and in vivo<sup>7,8</sup>. Our recent finding that the prolonged half-life of asparaginase in a pediatric patient suffering from ALL could be attributed to a germline mutation in the cathepsin B<sup>8</sup>, is now further supported by the in vitro and in vivo experiments presented here. Since lysosomal processing of epitopes is a crucial step towards successful antigen presentation, blocking cathepsin B mediated degradation by altering the amino acid sequence of asparaginase may enhance the therapeutic efficacy of this drug by reducing the immunogenicity.

We have limited our studies to *E.coli* asparaginase. Two other formulations are in use in clinic practice. *Erwinia chrysanthemi* asparaginase is frequently used as a second line treatment option after development of inhibitory antibodies. In our previous study<sup>8</sup>, we showed that the kinetics of *E.coli* and *Erwinia* asparaginase are similarly affected by a mutation in cathepsin B. In addition to its native form, a PEGylated form of *E.coli* asparaginase, which was introduced to reduce hypersensitivity reactions to the drug, is widely used in the clinic. The PEG coat reduced the immunogenicity due to its shielding properties: it inhibits direct, primarily charge mediated, binding of the protein to cells and prevents opsonization. Indeed, patients treated with PEG-asparaginase develop anti-asparaginase antibodies less frequently than patients treated with the native form<sup>20</sup>. Another most welcome effect of the PEGylation of asparaginase, is the prolonged half-life of this modified drug. This is consistent with our findings that the interaction between asparaginase and phagocytic cells is a critical determinant of the pharmacokinetics.

With an increased use of PEGylated drugs, not limited to asparaginase, it has become clear that patients do develop anti-PEG antibodies and that this can compromise therapeutic efficacy<sup>21-24</sup>. Therefore, use of PEG-asparaginase should also be supported by therapeutic drug monitoring to prevent underexposure<sup>25</sup> and as a result, the benefits compared to the use of native asparaginase are reduced.

Several studies have shown that the structure of asparaginase permits the introduction of modifications without appreciable loss of enzymatic function <sup>7, 26, 27</sup>. The data we present here may provide a rationale for the generation of novel modified versions of asparaginase that may no longer require PEGylation. Since our data show that phagocytic cells are an important sink for asparaginase as well as a key determinant of the asparaginase pharmacokinetics, preventing these interactions, by other means than PEGylation, could be of potential benefit. A modified form of asparaginase that exhibits a reduced affinity for such macrophage receptors is expected to have a prolonged half-life, show delayed clearance from the bone marrow and thus enhanced therapeutic efficacy.

In addition, we have shown that lysosomal protease cathepsin B is required for the efficient degradation of asparaginase by macrophages. Our in vivo studies demonstrate that loss of cathepsin B leads to a significantly prolonged asparaginase half-life in vivo, while inhibition of cathepsin B activity completely abolishes its degradation in vitro. While the incomplete depletion of phagocytic cells may explain the partial block of asparaginase turnover in the clodronate-treated mice, why cathepsin B knockout mice only display a delayed clearance, remains unclear. However, these results are in accordance with our previous report, which linked a germline loss-of-function mutation in the gene encoding cathepsin B to a prolonged serum half-life of asparaginase in a pediatric patient <sup>8</sup>.

## **Conclusions**

By using microSPECT/CT we showed that asparaginase is efficiently cleared by macrophages of the MPS. In particular, bone marrow resident macrophages may provide a protective environment for leukemic cells by effectively removing the therapeutic protein from the bone marrow niche. We conclude that cathepsin B is required for the degradation of asparaginase by macrophages, and that this degradation aids in the regulation of serum half-life. These new insights into both the prominent role of macrophages and the importance of the lysosomal protease cathepsin B in asparaginase clearance may aid in a rational design of a next generation asparaginase.

## References

1. Pieters R, Hunger SP, Boos J, et al. L-asparaginase treatment in acute lymphoblastic leukemia: a focus on Erwinia asparaginase. *Cancer*. Jan 15 2011;117(2):238-249.
2. Ehsanipour EA, Sheng X, Behan JW, et al. Adipocytes cause leukemia cell resistance to L-asparaginase via release of glutamine. *Cancer Res*. May 15 2013;73(10):2998-3006.
3. Iwamoto S, Mihara K, Downing JR, Pui CH, Campana D. Mesenchymal cells regulate the response of acute lymphoblastic leukemia cells to asparaginase. *J Clin Invest*. Apr 2007;117(4):1049-1057.
4. Tong WH, Pieters R, Hop WC, Lanvers-Kaminsky C, Boos J, van der Sluis IM. No evidence of increased asparagine levels in the bone marrow of patients with acute lymphoblastic leukemia during asparaginase therapy. *Pediatr Blood Cancer*. Feb 2013;60(2):258-261.
5. Steiner M, Hochreiter D, Kasper DC, et al. Asparagine and aspartic acid concentrations in bone marrow versus peripheral blood during Berlin-Frankfurt-Munster-based induction therapy for childhood acute lymphoblastic leukemia. *Leuk Lymphoma*. Sep 2012;53(9):1682-1687.
6. Brueck M, Koerholz D, Nuernberger W, Juergens H, Goebel U, Wahn V. Elimination of L-asparaginase in children treated for acute lymphoblastic leukemia. *Dev Pharmacol Ther*. 1989;12(4):200-204.
7. Patel N, Krishnan S, Offman MN, et al. A dyad of lymphoblastic lysosomal cysteine proteases degrades the antileukemic drug L-asparaginase. *J Clin Invest*. Jul 2009;119(7):1964-1973.
8. van der Meer LT, Waanders E, Levers M, et al. A germ line mutation in cathepsin B points toward a role in asparaginase pharmacokinetics. *Blood*. Nov 6 2014;124(19):3027-3029.
9. Halangk W, Lerch MM, Brandt-Nedelev B, et al. Role of cathepsin B in intracellular trypsinogen activation and the onset of acute pancreatitis. *J Clin Invest*. Sep 2000;106(6):773-781.



10. van der Have F, Vastenhouw B, Ramakers RM, et al. U-SPECT-II: An Ultra-High-Resolution Device for Molecular Small-Animal Imaging. *J Nucl Med*. Apr 2009;50(4):599-605.
11. Terry SY, Abiraj K, Lok J, et al. Can <sup>111</sup>In-RGD2 monitor response to therapy in head and neck tumor xenografts? *J Nucl Med*. Nov 2014;55(11):1849-1855.
12. Terry SY, Boerman OC, Gerrits D, et al. In-anti-F4/80-A3-1 antibody: a novel tracer to image macrophages. *Eur J Nucl Med Mol Imaging*. Aug 2015;42(9):1430-1438.
13. Chiu M, Franchi-Gazzola R, Bussolati O, D'Amico G, Dell'Acqua F, Rizzari C. Asparagine levels in the bone marrow of patients with acute lymphoblastic leukemia during asparaginase therapy. *Pediatr Blood Cancer*. Nov 2013;60(11):1915.
14. Tiziani S, Kang Y, Harjanto R, et al. Metabolomics of the tumor microenvironment in pediatric acute lymphoblastic leukemia. *PLoS One*. 2013;8(12):e82859.
15. Dimitriou H, Choulaki C, Perdikogianni C, Stiakaki E, Kalmanti M. Expression levels of ASNS in mesenchymal stromal cells in childhood acute lymphoblastic leukemia. *Int J Hematol*. Mar 2014;99(3):305-310.
16. Zhang W, Trachootham D, Liu J, et al. Stromal control of cystine metabolism promotes cancer cell survival in chronic lymphocytic leukaemia. *Nat Cell Biol*. Mar 2012;14(3):276-286.
17. Rennen HJ, Makarewicz J, Oyen WJ, Laverman P, Corstens FH, Boerman OC. The effect of molecular weight on nonspecific accumulation of (<sup>99m</sup>T)-labeled proteins in inflammatory foci. *Nucl Med Biol*. May 2001;28(4):401-408.
18. Brinkhuis RP, Stojanov K, Laverman P, et al. Size dependent biodistribution and SPECT imaging of (<sup>111</sup>In)-labeled polymersomes. *Bioconjug Chem*. May 16 2012;23(5):958-965.
19. Aderem A, Underhill DM. Mechanisms of phagocytosis in macrophages. *Annu Rev Immunol*. 1999;17:593-623.
20. Avramis VI, Sencer S, Periclou AP, et al. A randomized comparison of native *Escherichia coli* asparaginase and polyethylene glycol conjugated asparaginase for treatment of children with

- newly diagnosed standard-risk acute lymphoblastic leukemia: a Children's Cancer Group study. *Blood*. Mar 15 2002;99(6):1986-1994.
21. Armstrong JK, Hempel G, Koling S, et al. Antibody against poly(ethylene glycol) adversely affects PEG-asparaginase therapy in acute lymphoblastic leukemia patients. *Cancer*. Jul 1 2007;110(1):103-111.
  22. Richter AW, Akerblom E. Polyethylene glycol reactive antibodies in man: titer distribution in allergic patients treated with monomethoxy polyethylene glycol modified allergens or placebo, and in healthy blood donors. *Int Arch Allergy Appl Immunol*. 1984;74(1):36-39.
  23. Verhoef JJ, Carpenter JF, Anchordoquy TJ, Schellekens H. Potential induction of anti-PEG antibodies and complement activation toward PEGylated therapeutics. *Drug Discov Today*. Dec 2014;19(12):1945-1952.
  24. Garay RP, El-Gewely R, Armstrong JK, Garratty G, Richette P. Antibodies against polyethylene glycol in healthy subjects and in patients treated with PEG-conjugated agents. *Expert Opin Drug Deliv*. Nov 2012;9(11):1319-1323.
  25. Tong WH, Pieters R, Kaspers GJ, et al. A prospective study on drug monitoring of PEGasparaginase and Erwinia asparaginase and asparaginase antibodies in pediatric acute lymphoblastic leukemia. *Blood*. Mar 27 2014;123(13):2026-2033.
  26. Offman MN, Krol M, Patel N, et al. Rational engineering of L-asparaginase reveals importance of dual activity for cancer cell toxicity. *Blood*. Feb 3 2011;117(5):1614-1621.
  27. Verma S, Mehta RK, Maiti P, Rohm KH, Sonawane A. Improvement of stability and enzymatic activity by site-directed mutagenesis of E. coli asparaginase II. *Biochim Biophys Acta*. Jul 2014;1844(7):1219-1230.

Figure 1A

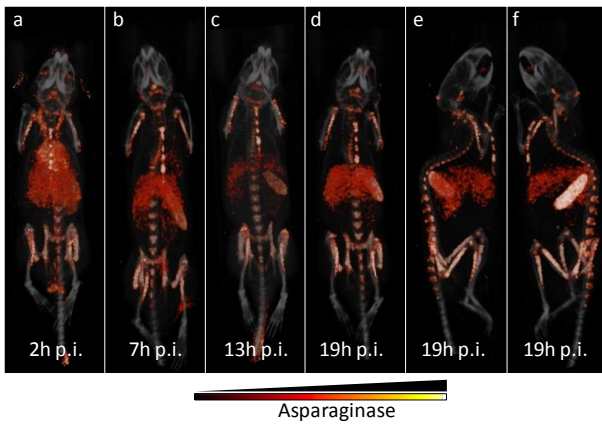


Figure 1B

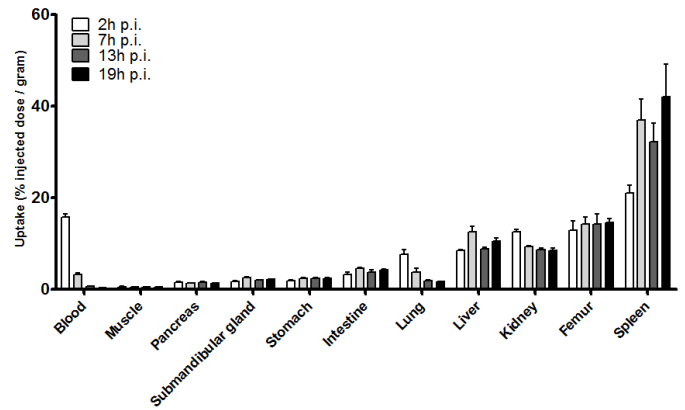


Figure 1C

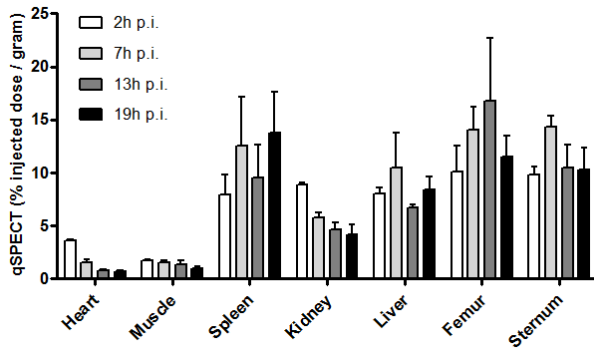
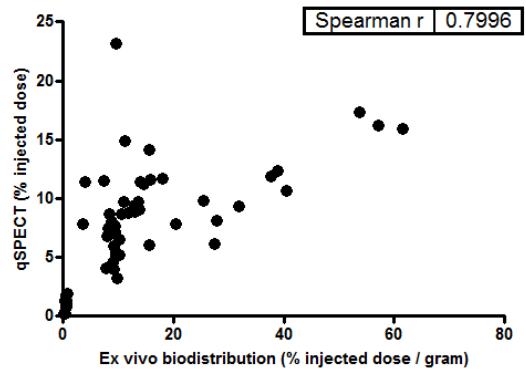


Figure 1D



**FIGURE 1. Asparaginase rapidly accumulates in spleen, liver and bone marrow**

**A** Ventral (a-d) and lateral (e,f) 3-dimensional volume projections of fused SPECT/CT scans of mice injected with <sup>111</sup>Indium-labeled asparaginase at the indicated hours post injection (h.p.i.).

**B** Ex vivo quantification of <sup>111</sup>Indium-labeled asparaginase uptake in various organs at the indicated hours post injection (h.p.i.). Data represent mean ± SEM of n = 5 mice per timepoint.

**C** Biodistribution of asparaginase as quantified from SPECT images. N=3 per timepoint.

**D** Uptake of <sup>111</sup>Indium-labeled asparaginase as quantified from micro-SPECT images plotted against values derived from ex vivo biodistribution studies.

Figure 2A

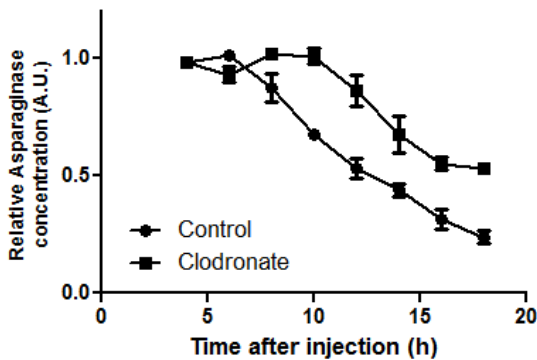


Figure 2B

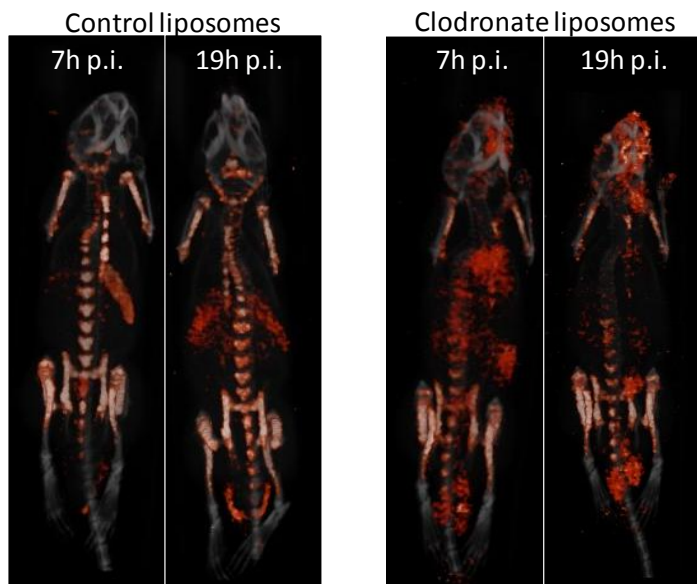
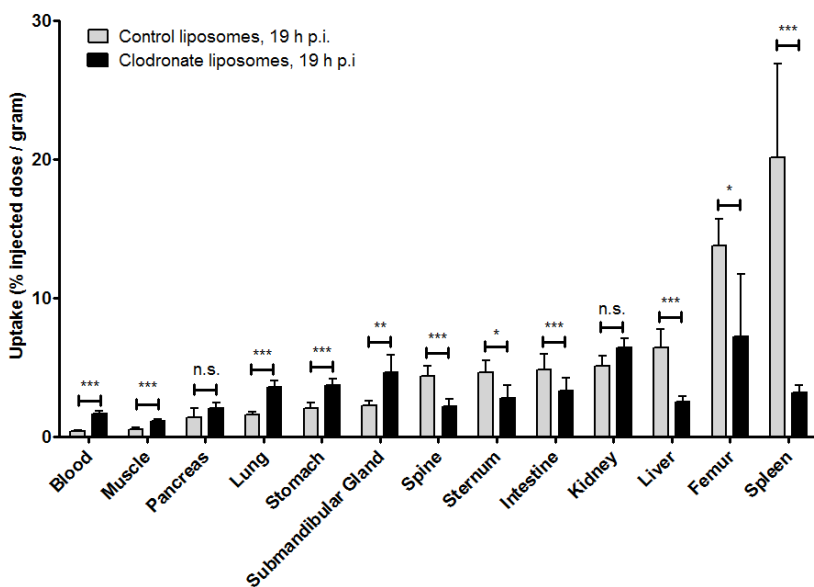


Figure 2C



**FIGURE 2. Depletion of macrophages affects asparaginase pharmacokinetics and biodistribution**

**A** Residual serum asparaginase activity at the indicated times after injection in mice. Mice were treated with a single dose of control or clodronate liposomes 24 hours prior to the asparaginase injection. At the indicated times after injection of unlabelled asparaginase, serum samples were taken and asparaginase activity was determined as described in the methods section. Data represent mean  $\pm$  SEM of  $n = 3$  mice per time point per treatment group. ANOVA statistical analysis was applied to test for significance.

**B** Ventral 3-dimensional volume projections of fused SPECT/CT scans of mice treated with a single dose of control or clodronate liposomes 24 hours prior to the <sup>111</sup>Indium-labeled asparaginase injection. Scans were made at 7 or 19 hours post injection (h p.i.) with <sup>111</sup>Indium-labeled asparaginase.

**C** Ex vivo quantification of <sup>111</sup>Indium-labeled asparaginase uptake in various organs of mice pretreated with control or clodronate liposomes, 19 hours post injection (h p.i.) of asparaginase. Data represent mean  $\pm$  SEM of  $n = 5$  mice per time point per treatment group. Statistical significance was determined by unpaired two-sided t-test. \* =  $p < 0.05$ , \*\* =  $p < 0.01$ , \*\*\* =  $p < 0.001$ .

Figure 3A

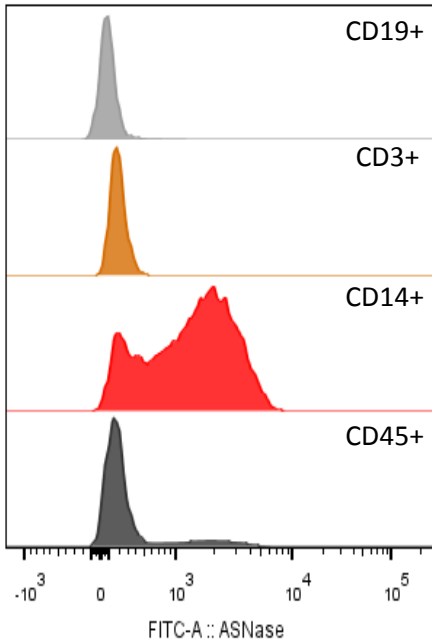


Figure 3B

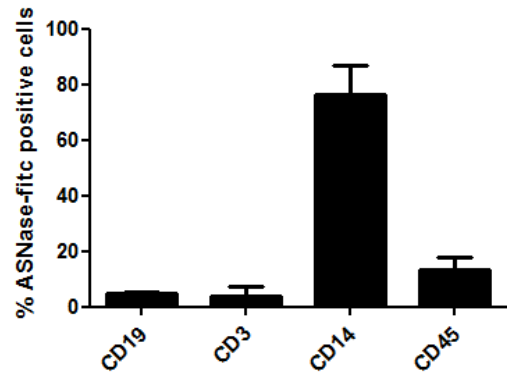
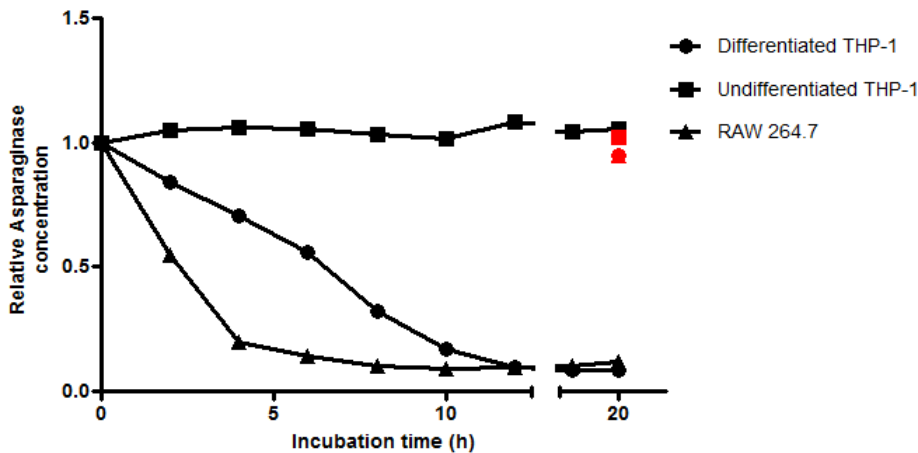


Figure 3C



**FIGURE 3. Human macrophages bind and degrade asparaginase**

**A** Histograms showing binding of asparaginase to various cellular subsets in PBMCs. Freshly isolated PBMCs were incubated with FITC-labelled asparaginase and subsequently identified based on the indicated cell surface markers using flowcytometry. Lineages were defined as follows: CD45-all nucleated cells, CD14-macrophages, CD3-T cells, CD19-B cells.

**B** Average of percentage of PBMC subsets binding FITC-labeled asparaginase (N=2).

**C** Asparaginase degradation in lysates of cell lines. Asparaginase was incubated in lysate of human undifferentiated, monocyte like THP-1 cells (squares), differentiated, macrophage like THP-1 cells (circles) and the murine macrophage cell line RAW264.7 (triangles). After incubation, residual ASNase activity was assayed as described in the methods section. Cathepsin inhibitor CA-074 was included to selected samples to confirm the contribution of Cathepsin B in this degradation (red data points).

Figure 4A

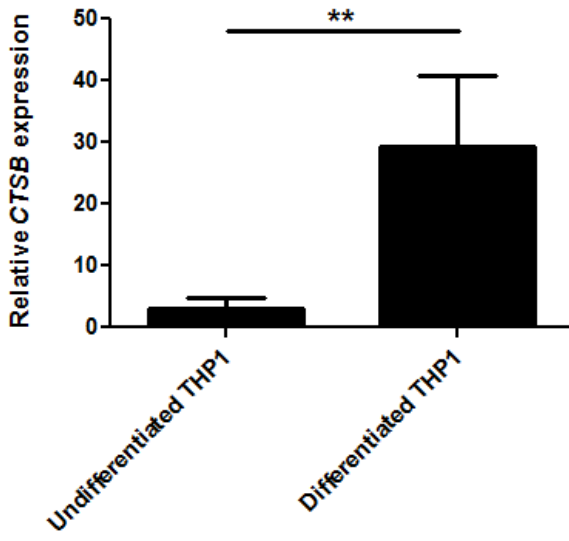


Figure 4B

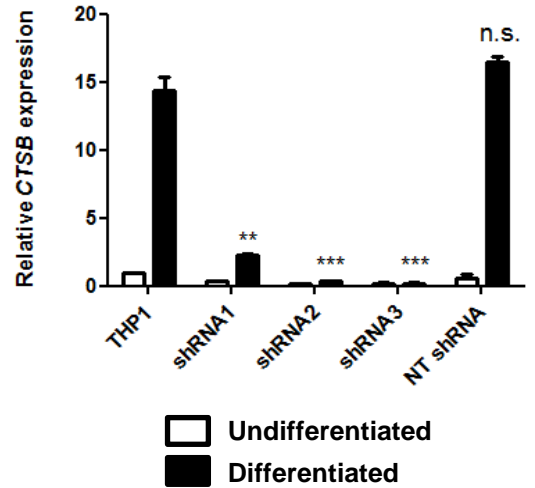


Figure 4C

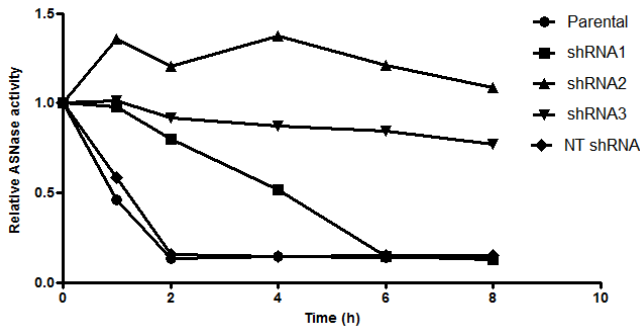
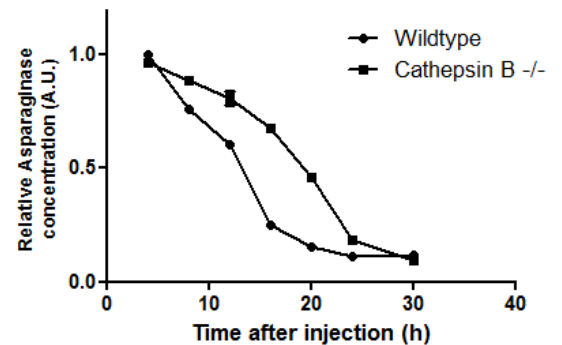


Figure 4D



**FIGURE 4. Cathepsin B is required for asparaginase degradation and controls asparaginase pharmacokinetics**

**A** Realtime quantitative PCR analysis of Cathepsin B mRNA expression in undifferentiated and PMA induced differentiated THP-1 cells, normalized for expression of TATA binding protein. Data represent mean  $\pm$  SEM of  $n = 4$ . Statistical significance was determined by unpaired two-sided t-test. \*\* =  $p < 0.01$ .

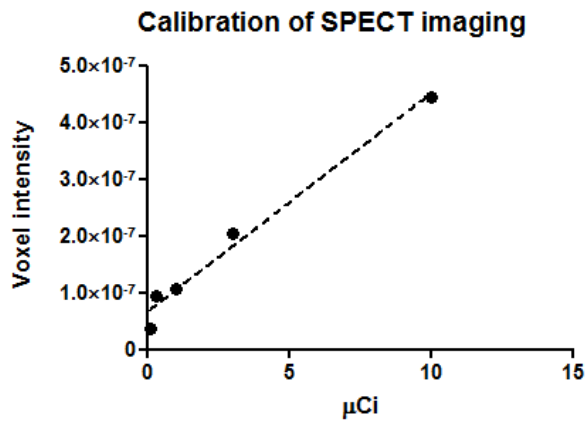
**B** Realtime quantitative PCR analysis of Cathepsin B mRNA expression in undifferentiated and PMA induced differentiated THP-1 cells transduced with shRNAs targeting Cathepsin B or control, non-targeting (NT) shRNA. Data are normalized for TBP expression and shown as mean  $\pm$  standard deviation of  $n = 2$ . Statistical significance was determined by unpaired two-sided t-test. \*\* =  $p < 0.01$ .

**C** Asparaginase degradation in lysates of cell lines. Asparaginase was incubated in lysate of differentiated THP-1 cells, transduced with control of Cathepsin B targeting shRNAs. After incubation, residual ASNase activity was assayed as described in the methods section. A representative example of multiple experiments ( $N=3$ ) is shown.

**D** Residual serum asparaginase activity at the indicated times after injection in mice. Cathepsin B knockout mice and age and sex matched control were injected with unlabelled asparaginase. At the indicated times after injection of unlabelled asparaginase, serum samples were taken and asparaginase activity was determined as described in the methods section. Data represent mean  $\pm$  standard deviation of  $n = 2$  mice per time point per treatment group. ANOVA statistical analysis was applied to test for significance.

# Supplemental Figures

S1

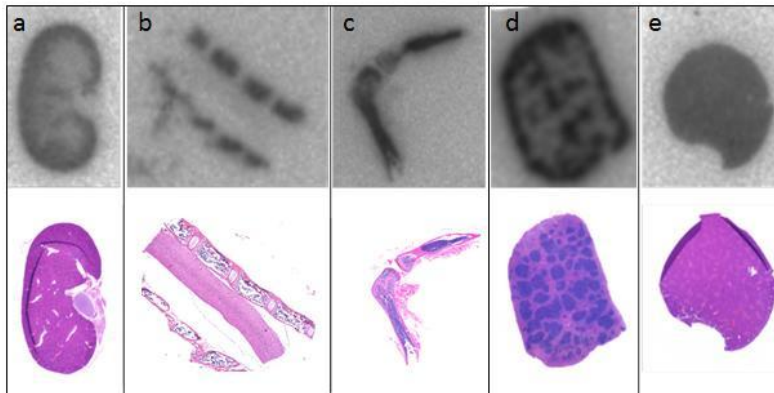


## Supplemental Figure 1. Calibration of qSPECT quantification

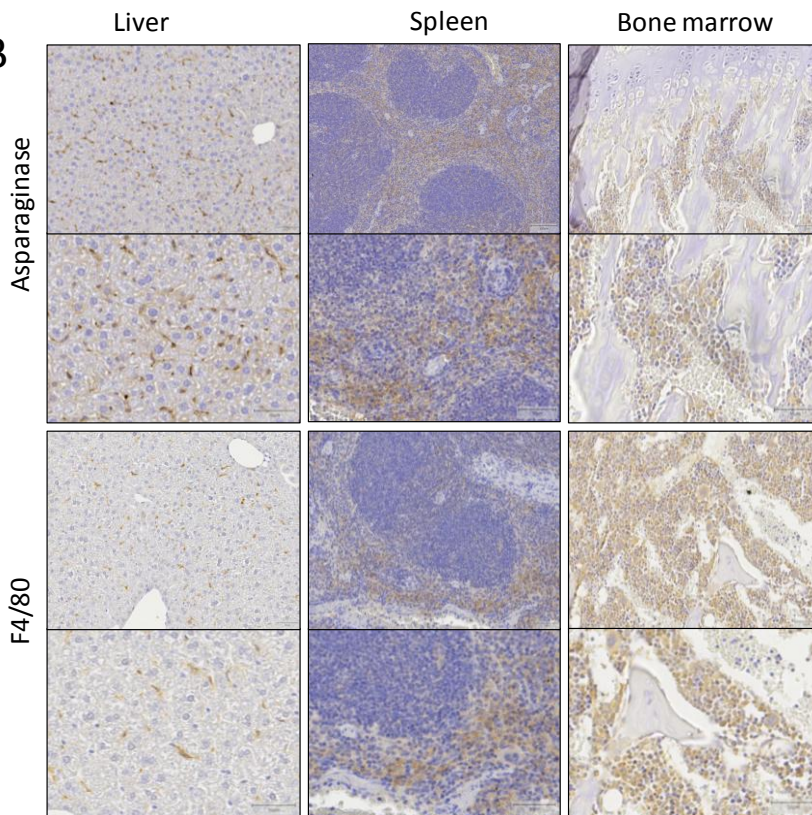
Calibration curve of a dilution series of <sup>111</sup>Indium-labeled asparaginase, determining the voxel intensity per µCi of activity.

## Supplemental Figures

S2A



S2B



**Supplemental Figure 2. Asparaginase is taken up in macrophage-rich parts of spleen, liver and bone marrow**  
**S2A** Autoradiography (upper image) and hematoxylin and eosin stain staining (lower image) of <sup>111</sup>Indium-labeled asparaginase. Images show kidney (a), spine (b), hind leg bones (c), spleen (d) and liver (e).

**S2B** Immunohistochemical staining of asparaginase and macrophage marker F4/80 in organs dissected from mice 9-15 hours post injection of unlabelled asparaginase. Images show two representative magnifications of liver, spleen and femoral bone marrow.

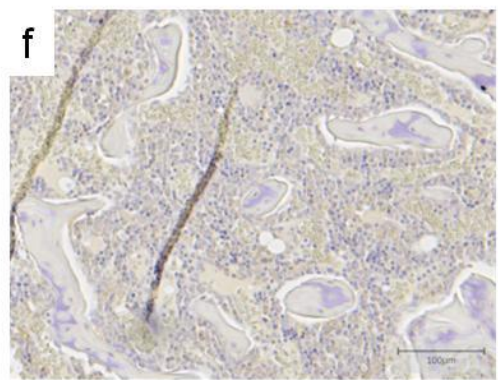
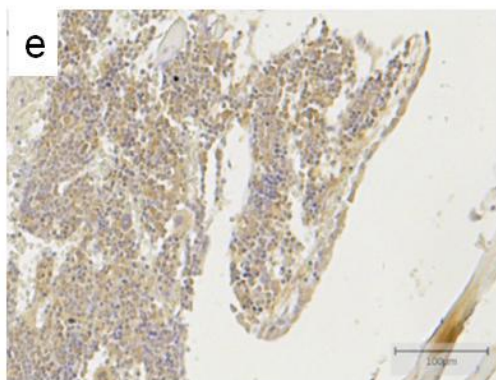
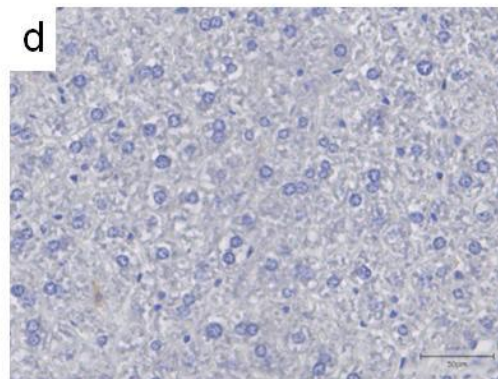
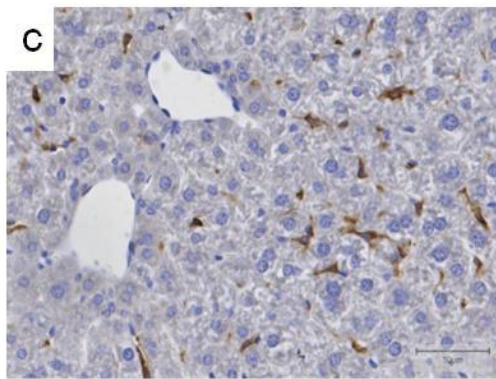
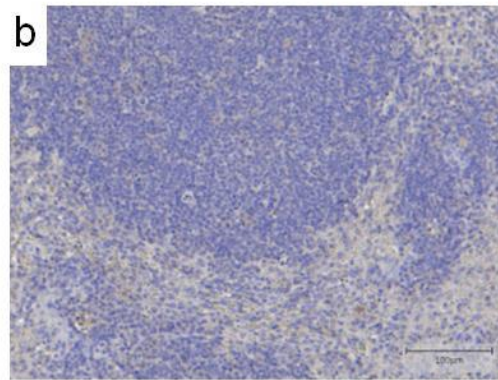
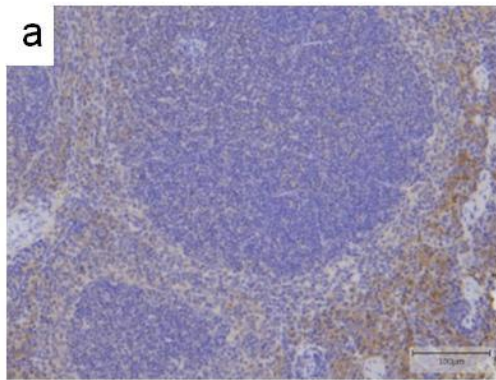


# Supplemental Figures

S3

Control

Clodronate

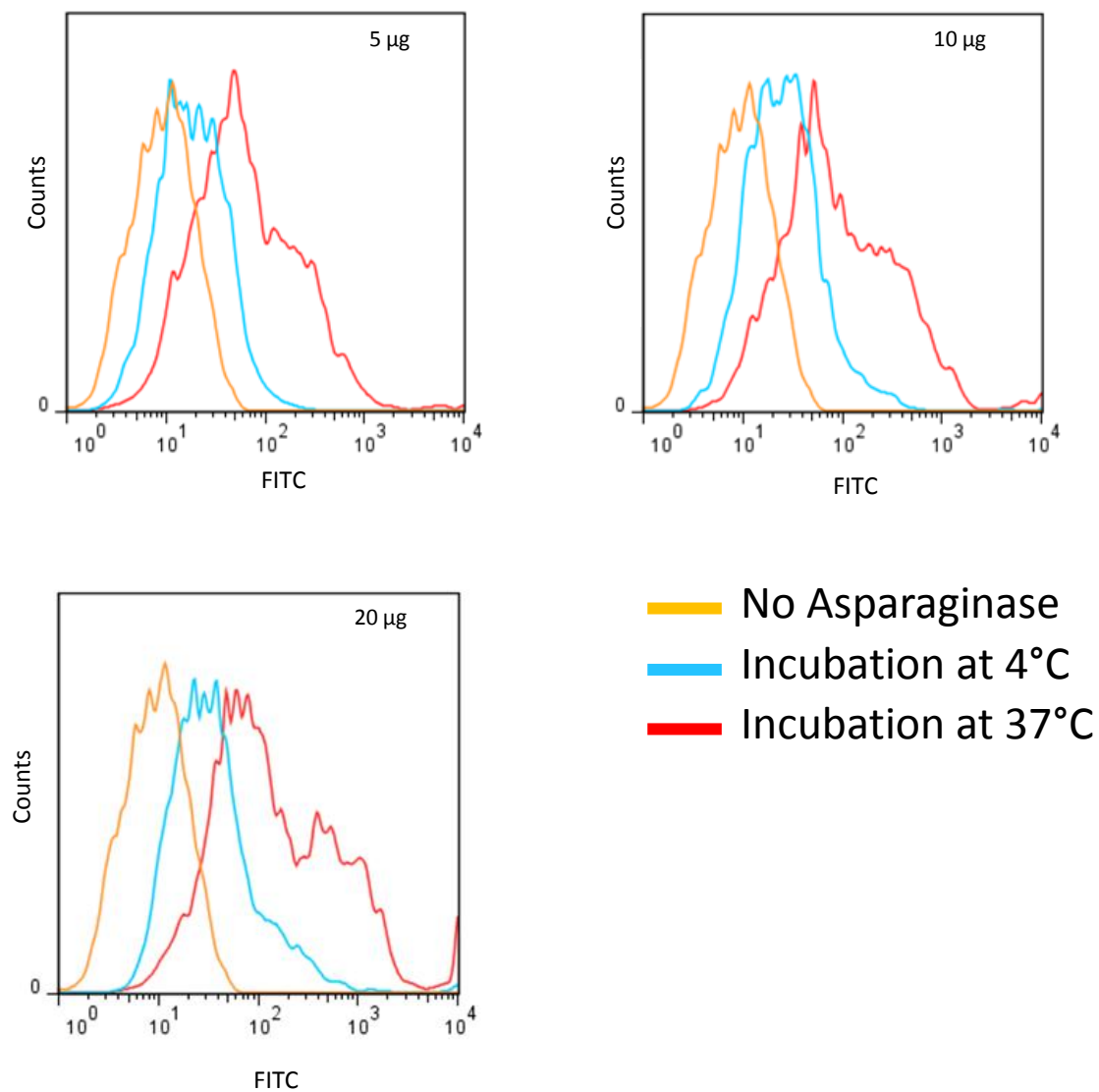


### Supplemental Figure 3. Immunohistochemical analysis of clodronate mediated macrophage depletion

Immunohistochemical staining of macrophage marker F4/80 in organs dissected from mice 9-15 hours post injection of control and clodronate liposomes. Representative images of, spleen (a and b) liver (c and d) and femoral bone marrow (e and f) are shown.

# Supplemental Figures

S4

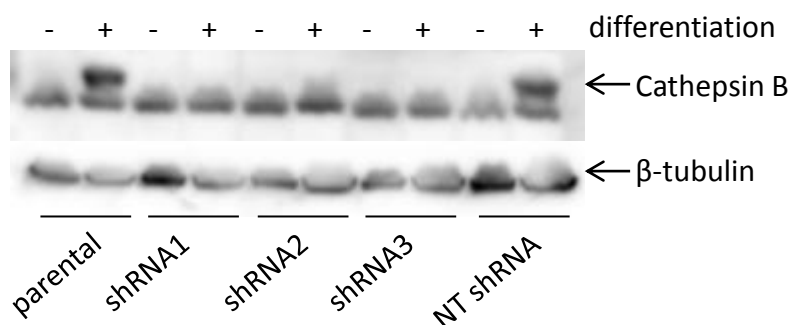


## Supplemental Figure 4. Differentiated THP1 cells bind asparaginase

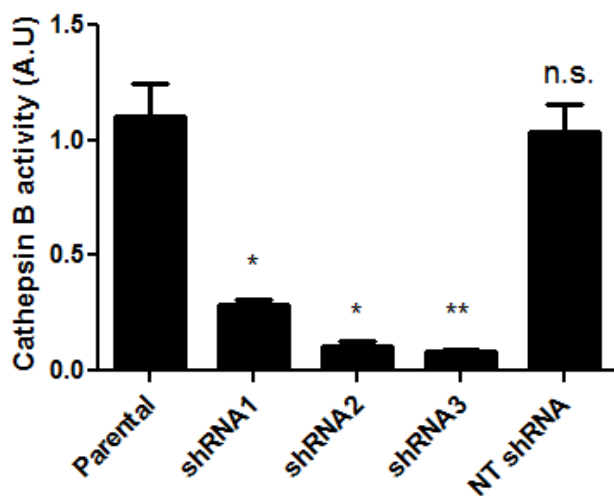
Histograms showing binding of asparaginase to differentiated THP-1 cells. PMA induced differentiated cells were incubated with different concentrations of FITC-labeled asparaginase at different temperatures. Binding was analyzed by flowcytometry.

## Supplemental Figures

### S5A



### S5B



#### Supplemental Figure 5. Cathepsin B protein expression and activity in THP-1 cells

**A** Western blot analysis of Cathepsin B protein expression in undifferentiated and PMA induced differentiated THP-1 cells transduced with shRNAs targeting Cathepsin B or control, non-targeting (NT) shRNA.  $\beta$ -tubulin was used as a control for equal loading.

**B** Cathepsin B activity in lysates of differentiated THP-1 cells transduced with control or Cathepsin B targeting shRNAs, was determined by measuring cleavage of the fluorescent substrate Ac-RR-AFC. The plot shows an average of 2 experiments with standard deviation. One of the control samples was set to 1 and all samples were correlated to this sample. Unpaired two-tailed t-test was used to determine significance compared to parental cells \* =  $p < 0.05$ , \*\* =  $p < 0.01$ .

## Supplemental tables

### Supplemental Table 1

Sequences of the shRNA constructs. Seed sequences are underlined.

shRNA	Hairpin sequence
Non-targeting shRNA	CACCCAACAAGATGAAGAGCACCAACGAAT <u>TGGTGCTCTTCATCTTGTTG</u>
Cathepsin B shRNA #1	CCGGCCAGAGAGTTATGTTTACCGACTCGAGT <u>CGGTAAACATAACTCTCTGGTTTT</u> T
Cathepsin B shRNA #2	CCGGGACAAGCACTACGGATACAATCTCGAGAT <u>TGTATCCGTAGTGCTTGCTTTT</u> T
Cathepsin B shRNA #3	CCGGCCAACACGTCACCGGAGAGATCTCGAGAT <u>CTCTCCGGTGACGTGTTGGTTTT</u> T

### Supplemental table 2

Sequences of RT-qPCR primers

Gene		Sequence
<i>CTSB</i> (human)	Forward	CTGAAGAGGCTATGTGGTACC
	Reverse	CCCTGGTCTCTGATCTCTTTG
<i>TBP</i> (human)	Forward	GCACAGGAGCCAAGAGTGAA
	Reverse	ACATCACAGCTCCCCACCAT
<i>Ctsb</i> (mouse)	Forward	ACAAGCCTTCCTCCACCCG
	Reverse	TGCCTCACCGAACGCAACC
<i>Hprt</i> (mouse)	Forward	GGGGGCTATAAGTTCTTTGCTGACC
	Reverse	TCCAACACTTCGAGAGGTCCTTTTCAC

## Supplemental methods

### Radiolabeling of asparaginase

Asparaginase (4 mg) was conjugated under strict metal-free conditions with isothiocyanatobenzyl–diethylenetriaminepentaacetic acid (ITC-DTPA, Macrocyclics, Dallas, TX) in 0.1 M NaHCO<sub>3</sub>, pH 9.5, using a 10-fold molar excess of ITC-DTPA. After 1 hour incubation at RT the conjugation mixture was dialyzed in a dialysis cassette with a molecular cut-off value of 20 kDa (Slide-A-Lyzer 20K, Thermo Scientific, Waltham, MA) against 0.25 M Ammonium Acetate, pH 5.5 to remove the unconjugated ITC-DTPA. The substitution ratio, as determined by labeling the conjugation mixture with <sup>111</sup>InCl<sub>3</sub> (600-800 MBq, Mallinckrodt, Petten, The Netherlands), was 0.8 DTPA/asparaginase molecule. <sup>111</sup>InCl<sub>3</sub> was added to DTPA-asparaginase (50-65 µg) for 1 h at RT in 0.1 M 2-(N-morpholino)ethanesulfonic acid buffer, pH 5.4. Free In-111 was complexed by adding 50 mM ethylenediaminetetraacetic acid (EDTA; final concentration of 5 mM). Quality control was performed using instant thin-layer chromatography. To obtain a radiochemical purity ≥95%, <sup>111</sup>In-labeled protein was purified by gel filtration on a disposable PD10 column (GE Healthcare Life Sciences, Eindhoven, the Netherlands), eluted with PBS containing 0.5% bovine serum albumin (BSA). The specific activity of the radiolabeled asparaginase preparations used in the experiments was (5-12 MBq/µg).

### Autoradiography

Formalin-fixed, paraffin-embedded tissue sections (4 µm) from mice injected intravenously with <sup>111</sup>In-asparaginase were dewaxed, rehydrated and exposed to a phosphor imaging screen for up to 7 days. The screen was scanned in a phosphor imager system (Bioimaging Analyzer System 1800-II; Fujifilm, Tilburg, the Netherlands) at a pixel size of 50 × 50 µm.

### **Asparaginase binding assay**

Human peripheral blood mononuclear cells (PBMCs) were isolated from blood obtained from healthy volunteers upon informed written consent, using density gradient centrifugation (Lymphoprep; Axis-Shield, Dundee, Scotland). Asparaginase (Takeda, Hoofddorp, the Netherlands) was conjugated with Fluorescein isothiocyanate according to manufacturer's instructions (Pierce / Life Technologies, Carlsbad, CA). PBMCs or THP-1 cells were incubated with FITC labeled asparaginase in culture medium for 1 hour at the indicated temperatures. After incubation, PBMCs were stained for expression of lineage markers with anti-CD14, -CD45, -CD3 and -CD19 antibodies purchased from BD Biosciences and analyzed using a LSRII flow cytometer (BD Biosciences, Breda, the Netherlands). The data were collected and analyzed by FlowJo software version 8.8.7 FlowJo, Ashland OR).

### **Immunohistochemistry**

For histological analysis, tissues and organs, including spleen, lymph nodes, thymus, liver and femur/tibia were fixed in 4% formalin during 24 hours. Bone containing tissues were decalcified using Osteosoft (Merck Laboratories). Specimens were embedded in paraffin, 4  $\mu$ M serial sections were cut and stained with hematoxylin and eosin (HE) following standard procedures. After dewaxing, rehydration and antigen retrieval using sodium citrate, slides were blocked with 2% normal goat serum (Vector Laboratories, Burlingame, CA) and 2% BSA in 0.05% PBS, Tween20 prior to overnight staining with F4/80 (MCA497GA, AbD Serotec, Oxford, United Kingdom) and Asparaginase (ab21013, Abcam, Cambridge, United Kingdom) antibodies. Appropriate biotinylated antibodies (Vector Laboratories) were used as secondary antibody and staining was revealed by incubation with metal-enhanced diaminobenzidine in stable peroxide substrate buffer (Thermo Fisher Scientific Inc.). After counterstaining with hematoxylin (1:3) slides were dehydrated and coverslipped using entellan

(Merck Laboratories). Images were captured using a VisionTek digital microscope (Sakura Finetek, Torrance, CA).

### **Cell culture**

The human acute monocytic leukemia cell line THP-1 was obtained from the American Type Culture Collection (ATCC, #TIB-202) cultured in RPMI 1640 containing L-glutamine (Invitrogen /Life technologies), supplemented with 10% heat-inactivated fetal bovine serum (Greiner Bio-One), and 100 units/ml penicillin/streptomycin (Invitrogen). The mouse leukemic monocyte macrophage cell line RAW264.7 (ATCC #TIB-71) and HEK293 FT (Invitrogen) cells were cultured in DMEM containing L-glutamine (Invitrogen), supplemented with 10% heat-inactivated fetal bovine serum, 100 units/ml penicillin/streptomycin, and 1% non-essential amino acids (Invitrogen). All cells were incubated at 37°C in a 5% CO<sub>2</sub> humidified atmosphere. All cell Lines were used within 3 months of culture. THP-1 differentiation was induced by culturing 5 – 8 x 10<sup>6</sup> cells in the presence of 100 nM phorbol myristate acetate (PMA; Sigma-Aldrich) for three days. After three days the medium was refreshed by medium without PMA and terminal differentiation was continued for an additional three days.

### **Real-time Quantitative Polymerase Chain Reaction**

Total RNA was extracted using the RNeasy mini-kit (Qiagen, Venlo, the Netherlands) according to manufacturer's instructions. Subsequently, cDNA was synthesized of 500 ng RNA template using the iScript™ cDNA synthesis kit (Bio-Rad, Hercules, CA). mRNA expression levels were determined by use of Power SYBR® Green PCR master mix using gene-specific primers (sequences are listed in Supplemental Table 2) and the CFX96 Touch™ Real-Time PCR detection system (Bio-Rad). TBP mRNA expression was used as a reference to obtain the relative fold expression of target genes using the comparative cycle threshold  $2^{(-\Delta\Delta Ct)}$  method. Prism software (Graphpad, La Jolla, CA) was used to plot the data and for statistical analysis.  $p < 0.05$  was considered a significant difference.

## **Immunoblotting**

Whole cell extracts were prepared in NP-40 lysis buffer (200 mM NaCl, 0.5% NP-40, 20 mM Tris-HCl, pH 8.0, 5 mM EDTA) and cleared by centrifugation. Protein lysates were resolved by sodium dodecyl sulfate polyacrylamide gel electrophoresis (SDS-PAGE) and transferred to a polyvinylidene difluoride (PVDF) membrane. The membranes were probed with primary antibodies against cathepsin B (sc-13985, Santa Cruz Biotechnology, Dallas, TX) or  $\beta$  tubulin (#2128, Cell Signalling Technology, Leiden, the Netherlands), followed by horseradish peroxidase (HRP) conjugated secondary antibody (DAKO, Heverlee, Belgium). Proteins were visualized with ECL reagent (GE Healthcare) and expression was detected with Fluorchem (Protein Simple, San Jose, CA).

## **References**

1. Terry SY, Boerman OC, Gerrits D, et al. In-anti-F4/80-A3-1 antibody: a novel tracer to image macrophages. *Eur J Nucl Med Mol Imaging*. Aug 2015;42(9):1430-1438.



Figure 1A

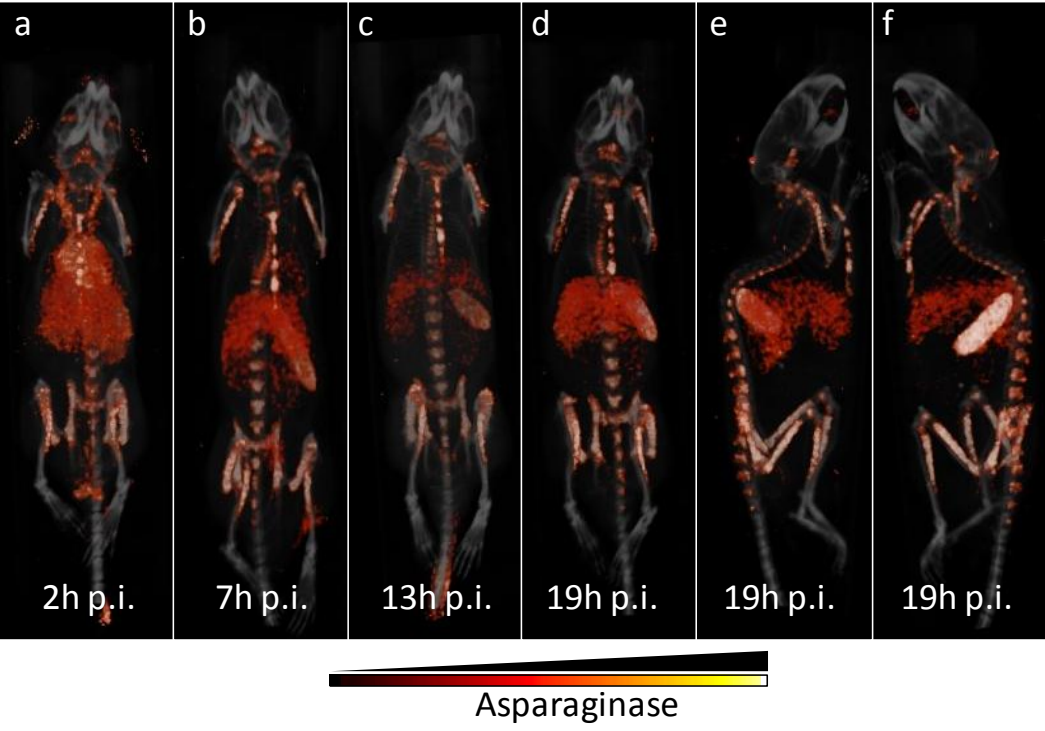


Figure 1B

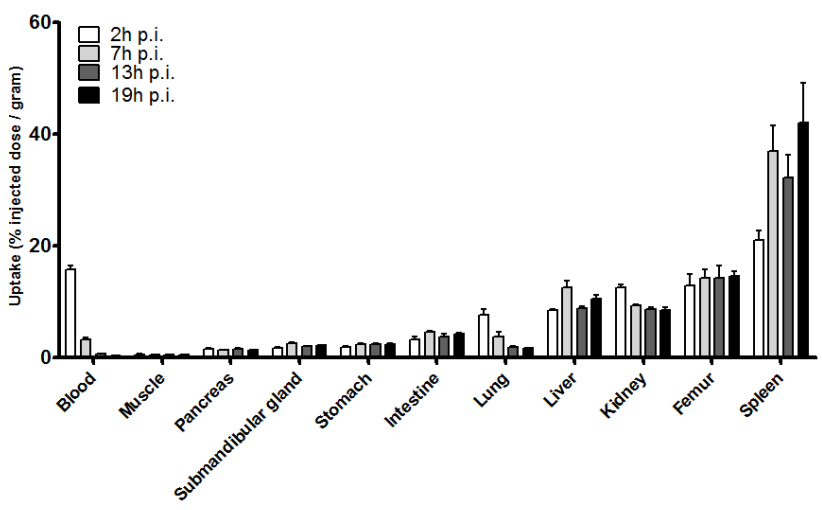


Figure 1C

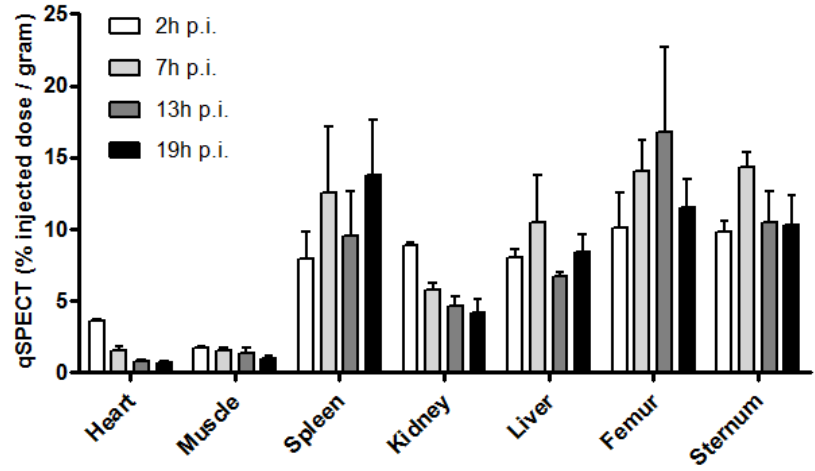


Figure 1D

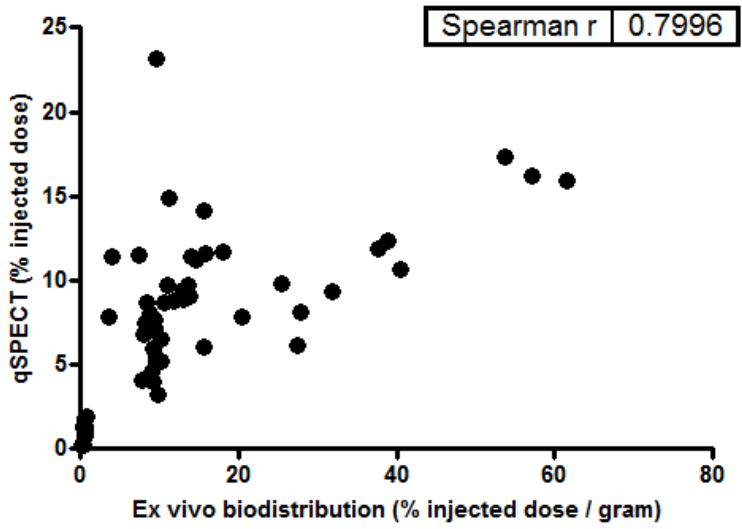


Figure 2A

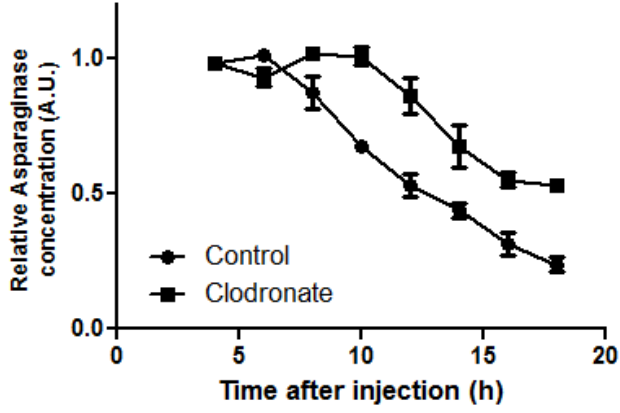


Figure 2B

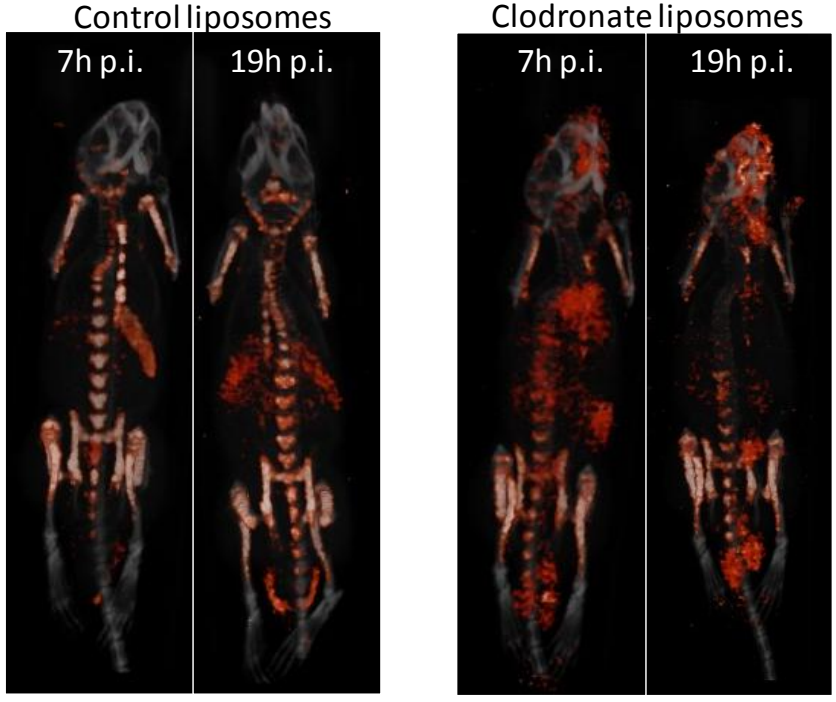


Figure 2C

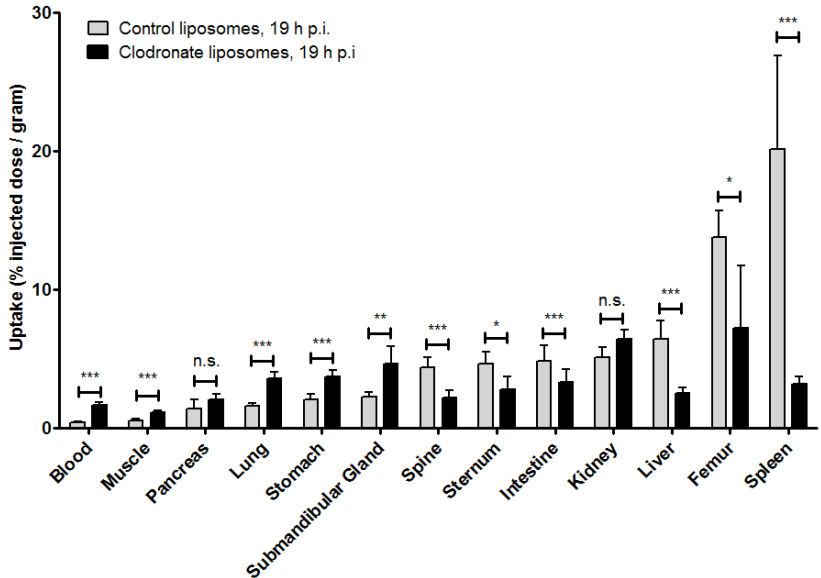


Figure 3A

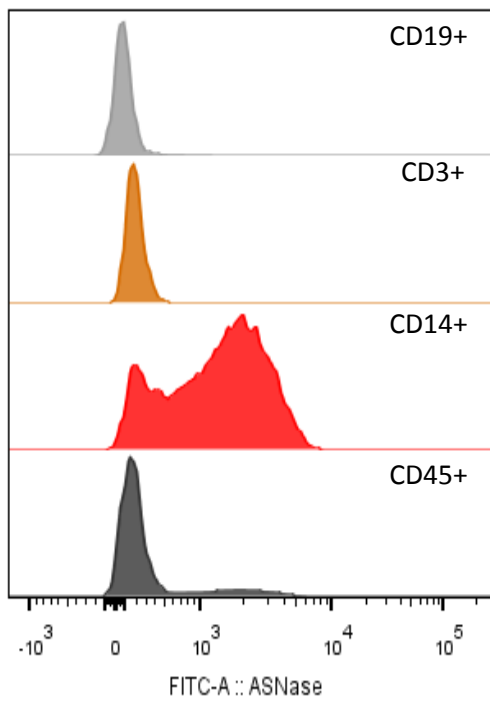


Figure 3B

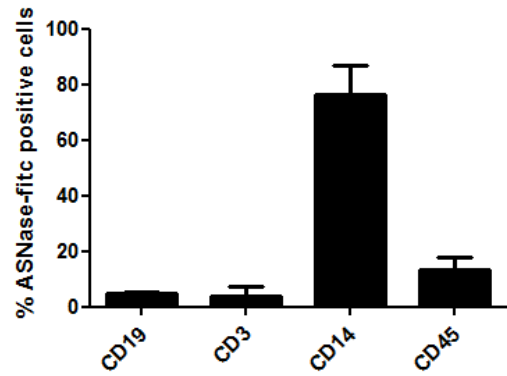


Figure 3C

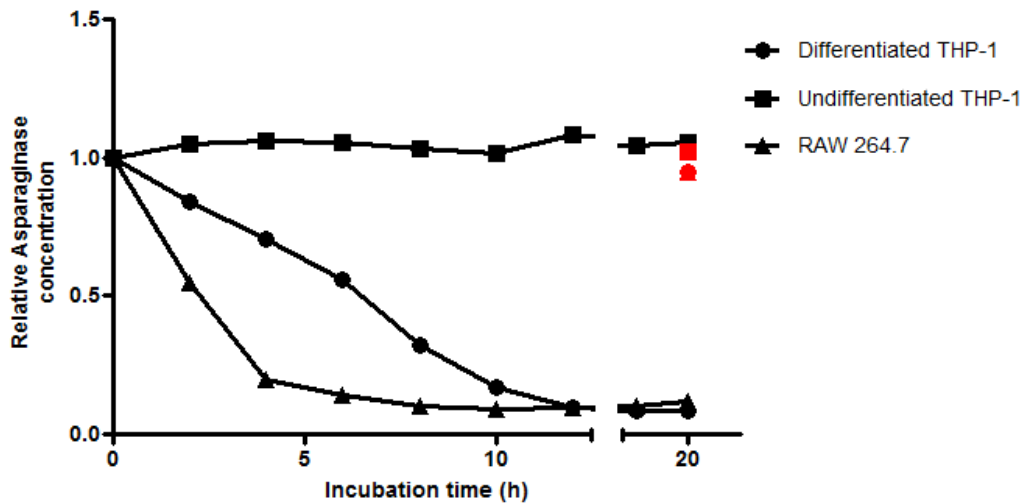


Figure 4A

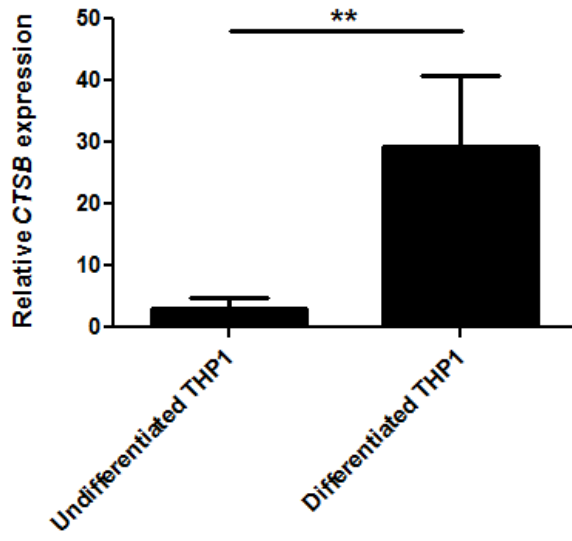


Figure 4B

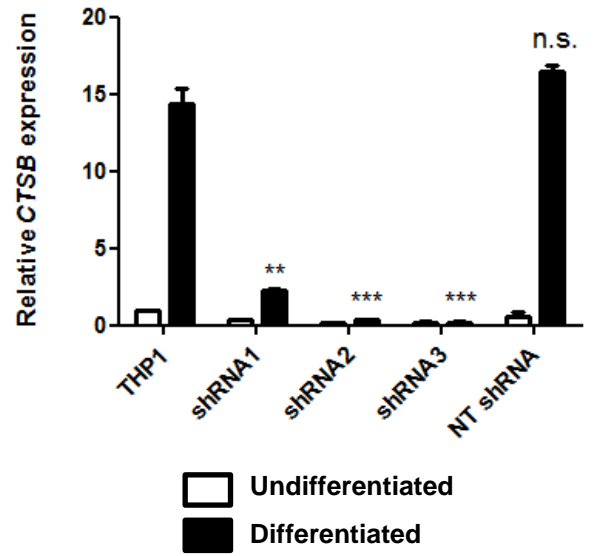


Figure 4C

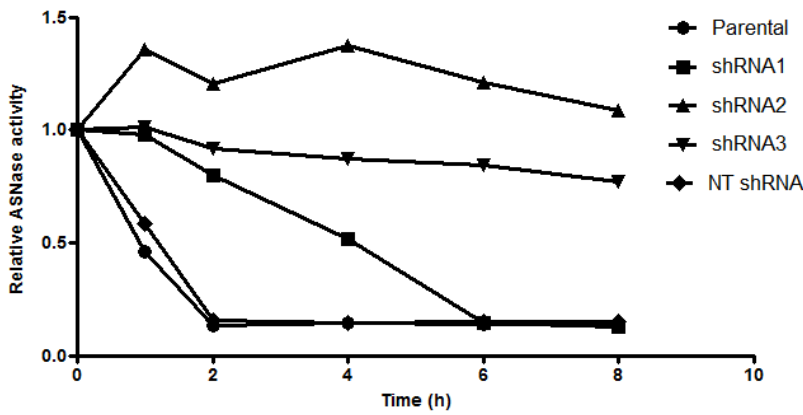


Figure 4D

